University of Glasgow
DEPARTMENT OF
AEROSPACE ENGINEERING

UNIVERSITY OF GLASGOW
2 1 NOV 1996
LIBRARY

Engineering
PERIODICALS
U5000

Chicago Beach Resort Development – An Assessment of the Transverse Galloping Stability of the Tower Hotel Mast.

by

M. Vezza

UNIVERSITY
of
GLASGOW

Chicago Beach Resort Development – An Assessment of the Transverse Galloping Stability of the Tower Hotel Mast.

by

M. Vezza

Department of Aerospace Engineering
University of Glasgow
Glasgow G12 8QQ.

on behalf of

W.S. Atkins and Partners Overseas.

G.U. Aero Report No. 9626
October 1996.

SUMMARY.

This report forms the second part of a study, commissioned by W.S. Atkins and Partners Overseas, into the galloping stability of the prismatic elements of the Tower Hotel, which is part of the Chicago Beach Resort Development. The particular subject of this study is the mast which extends above the top of the Hotel, which was not investigated previously due to a lack of relevant aerodynamic data.

The report presents aerodynamic data for a number of shapes which have been identified as possessing some of the important features of the the mast cross-section. Along with the structural and modal data supplied by W.S. Atkins, an assessment of the critical galloping speeds of these shapes is made after extending the quasi-steady theory originally described in the first report.

There is strong evidence to suggest that the mast will not experience an instability due to transverse galloping, however the absence of sharp corners increases significantly the sensitivity of the transverse force coefficient to body geometry and Reynolds number. Increased confidence in the assessment requires more accurate aerodynamic data, obtainable from a series of wind tunnel tests on representative scale models of the mast cross-section.

CONTENTS.

1. INTRODUCTION.

The Chicago Beach Resort Development is a planned new tourist resort, located approximately 15km from the centre of Dubai, United Arab Emirates. A recent report by Vezza (1996), which was commissioned by W.S. Atkins and Partners Overseas, provided an assessment of the transverse galloping stability of the external frame of the Tower Hotel, illustrated in Fig. 1.1. This previous report is subsequently referred to herein as "the Review".

The current report is the result of an additional investigation requested by W.S. Atkins of the galloping stability of the mast which extends from the top of the Tower Hotel, Fig 1.1. In the Review it was stated that an assessment of the galloping stability of the mast could not be made at that time because relevant aerodynamic data could not be found. Part of the current work was aimed at identifying shapes which , to some degree, approximate the actual cross-section of the mast and for which aerodynamic data exist. In the following sections the data are presented and calculations performed to enable an assessment of the mast stability to be made, from which conclusions are then drawn.

2. STRUCTURAL AND AERODYNAMIC DATA FOR THE MAST.

As indicated in the Review, no aerodynamic data have been found which correspond to the exact sectional geometry of the mast. However, a number af data sources have been identified which provide useful information on bodies with some degree of streamlining around the windward and leeward faces, and these are presented in this section.

2.1. Mast Geometry, Mass Distribution and Damping.

The mast arrangement is illustrated in Fig. 2.1 and extends over a total height of 114.6m from base to top with a 0.9° taper. Since the lower portion of the mast is rigidly braced, the upper portion is assumed to be cantilevered about section I for the purposes of the stability assessment, which reduces the flexible height to 60.65m. The basic form of the cross-section is given in Fig. 2.2, and the varying depth can be calculated from the given taper.

The mass distribution of the mast, supplied by W.S. Atkins, is given in Table 1 and is required for the stability calculation in section 3. Only the mass values above section I are required, and the average mass per unit length in each of the bays 1 to 6 (Fig. 2.1) is given.

The tuned mass damper is located immediately above section Q. With damper in place, a conservative estimate of the structural damping of the mast, based on information supplied, is 4% of critical damping. Should a higher figure be achieved in practice, this would be beneficial from a stability viewpoint, raising the critical galloping speed.

2.2. Geometric Approximations to the Mast Cross-Sections.

The mast is a long slender body of small taper ratio and hence will be influenced heavily by cross-sectional aerodynamics for a horizontal wind. Three-dimensional effects, in the form of spiral vortices generated from the exposed and swept tip, will be present but are not included in the calculations presented in section 3. However, as mentioned in the Review, there is some evidence to suggest that a two-dimensional assessment is conservative as far as galloping stability is concerned (Novak and Tanaka, 1974).

The application of quasi-steady theory to the assessment of high speed transverse galloping was described in the Review. This theory employs the static aerodynamic characteristics of the mast cross-section. The root and tip cross-sections of the cantilevered part of the mast are given by the solid lines in Fig. 2.3. The root corresponds to section I and the tip section is located 7.5m from the top. The crucial factor in high speed galloping is the shape of the shear layers emanating from the body, as these have a large influence on the pressure distribution and hence the aerodynamic loads. A number of different cross-sectional shapes have been identified as possessing some of the important features of the mast sections, and these are inscribed into the mast sections in Figs. 2.3(a) to 2.3(c).

A wide range of aerodynamic data are available for ellipses of different aspect ratios (ESDU, 1979), therefore ellipses can be chosen which match the mast sections as closely as possible, Fig. 2.3(a). The tip ellipse is a fairly good approximation to the tip section, which is the most important aerodynamically for vibration in the fundamental mode. The ellipse, however, possesses a smooth curvature distribution which is different from the mast around both the crucial leading edge region and the side faces, and this would alter the separation characteristics to some degree.

The mast sections can be formed from enveloping rectangles having rounded corners of radius to height ratio $r/h = 0.5$. No data on such shapes have been found, however aerodynamic data have been found for rectangles and squares for other limited radius ratios (Polhamus, 1958) and these are illustrated in Fig. 2.3(b). The rounded corners provide a basic similarity to the mast sections in that flow which would normally separate from sharp corners will remain attached around the corners to some degree , dependent on the Reynolds number, In addition the flattened sides of the mast sections are represented very well by the rounded quadrilaterals, therefore some insight into the actual mast aerodynamics may be provided, particularly at positive wind incidence.

The last approximate representation of the mast section is the shape formed from two eccentric circles, Fig. 2.3(c), which was tested as part of an investigation into the effects of ice accretion on cables (Richardson, 1986). The windward face is represented exactly with this shape, however the small eccentricity provides less fidelity in the geometric representation of the side faces, considering that the circle is completely stable in galloping.

2.3. Aerodynamic Data for the Various Cross-Sectional Approximations.

The sources of aerodynamic data referred to in section 2.2 have been processed to produce the transverse force versus incidence graphs illustrated in Fig. 2.4. The test conditions in all cases correspond to very low freestream turbulence intensities, hence the flow can be considered smooth. Based on the wind assessment reported by BMT Fluid Mechanics Ltd. (Coleman and Davies, 1994) the mast is exposed to a turbulence intensity of approximately 10%. However, as reported in the Review, neglecting turbulence is normally conservative with respect to galloping stability, hence the data are of value. The sign convention employed is illustrated in Fig. 2.5, and is identical to that in the Review. Although the transverse force coefficient is based on a wind at zero incidence to the body, values corresponding to a wind at any other incidence can easily be obtained, as explained in section 3. Unlike flow around sharp edged bodies, the separation points on bodies with rounded surfaces are not fixed for all flow conditions. The locations of the separation points, and hence the profile of the shear layers, are dependent on whether the flow is above or below a critical Reynolds number, which can be different for each body. The effect can be to drastically change the transverse force characteristic, even to the extent of changing sign, as illustrated in Fig. 2.6. Matching the Reynolds number zone operating in the test and site environment is therefore of utmost importance in this case. The data indicate that Reynolds number transition occurs somewhere between 10^5 and 10^6, based on section height, for the various cross-sectional shapes. For a wind speed of 10m/s the site Reynolds number is approximately given by:

$$\mathrm{Re} = \frac{\rho V h}{\mu} = \frac{1.2 \times 10 \times 2.5}{1.78 \times 10^{-5}} = 1.7 \times 10^{6}$$

where ρ and μ are the density and dynamic viscosity of air in kg/m^3 and kg/ms respectively. It can be assumed therefore that for all wind speeds of interest the data pertaining to the supercritical Reynolds number region are applicable. All of the data presented in Fig. 2.4. corresponds to the supercritical region unless stated otherwise, with the exception of the data for the shape formed from the eccentric circles. This shape was tested at the single Reynolds number of 105,000 , which is in the transition zone, and may not be totally representative of the site conditions.

One of the important parameters involved in the assessment of galloping stability, as explained in the Review, is the slope of the transverse force versus incidence graph. If this is positive anywhere then a potential for instability exists and should be investigated. Using this criterion it is evident that the elliptical sections are completely stable , possessing negative slopes at all incidence values. The force characteristics for the rounded quadrilateral sections do exhibit regions in which the slope is positive, between 15° and 25° incidence in particular, therefore a stability assessment is required and is provided in section 3. The subcritical square data is included to highlight the Reynolds number effect mention above, and it should be noted that this also indicates a potential stability problem in subcritical flow. The shape formed from the eccentric circles possesses a positive force slope between 8° and 16° incidence, but is stable at all other incidence values. However, a stability assessment is necessary and is provided in section 3.

3. ASSESSMENT OF THE GALLOPING STABILITY OF THE MAST.

The data presented in section 2 enable an assessment to be made of the critical galloping speed of the mast corresponding to the fundamental mode of vibration. The various cross-sections are analysed to provide a range of critical speed values from which conclusions are drawn.

3.1. Equivalent Mass of the Mast.

The mass distribution of the mast is not constant, as indicated in Table 1. The equivalent modal mass per unit length must therefore be used in the stability calculations. The fundamental mode shape for a tapered cantilever is closely approximated by a parabola, as indicated in Fig. 3.1. The equivalent mass per unit length, m_e, is given by:

$$m_e = \frac{\int_0^1 m[f(\xi)]^2 \, d\xi}{\int_0^1 [f(\xi)]^2 \, d\xi}$$

where $f(\xi)$ is the normalised mode shape and ξ is the non-dimensional position along the mast from the cantilevered root. The parabolic mode shape is given by $f(\xi) = \xi^2$. Note that both $f(\xi)$ and ξ are in the range [0,1]. Since $\int_0^1 [f(\xi)]^2 \, d\xi = 1/5$, the equivalent mass per unit length can be calculated from the expression:

$$m_e = \sum_{i=1}^{6} m_i \left(\xi_2^5 - \xi_1^5\right)_i$$

where ξ_1 and ξ_2 are the locations of the lower and upper bay boundaries, and the m_i values are obtained from Table 1. Performing the indicated calculation results in an equivalent mass per unit length of 1298kg/m. As expected the value of m_e is heavily weighted towards the tip mass values, due to the larger inertial effect in this region.

3.2. Transverse Galloping Speed at Non-Zero Wind Incidence.

The basic quasi-steady theory of transverse galloping for a wind at zero incidence was given in the Review. The situation is slightly altered for a wind at non-zero incidence, Fig. 3.2. The force coefficient referred to incident wind V at mean incidence $\overline{\alpha}$ is denoted $C_y^{\overline{\alpha}}$, and is related to the original force coefficient referred to the wind component at zero incidence, C_y, by the equation:

$$C_y^{\bar{\alpha}} = C_y \cos^2 \bar{\alpha}$$

$$\therefore \quad \frac{dC_y^{\bar{\alpha}}}{d\alpha} = \frac{dC_y}{d\alpha} \cos^2 \bar{\alpha}$$

At the initiation of oscillation the change in incidence , $\Delta\alpha$, is small and is given by $\Delta\alpha = \frac{\dot{y}}{V} \cos \bar{\alpha}$. The dynamic equation governing the initial motion is therefore:

$$m_e \ddot{y} + 2 m_e N \delta_s \dot{y} + k y \;=\; \frac{1}{2} \rho V^2 h \left. \frac{dC_y^{\bar{\alpha}}}{d\alpha} \right|_{\alpha=\bar{\alpha}} \Delta\alpha \;=\; \left(\frac{1}{2} \rho V h \cos^3 \bar{\alpha} \left. \frac{dC_y}{d\alpha} \right|_{\alpha=\bar{\alpha}} \right) \dot{y}$$

The critical galloping speed corresponds to zero nett damping, and is given by:

$$V_{crit} \;=\; \frac{4 m_e N \delta_s}{\rho h \cos^3 \bar{\alpha} \left. \frac{dC_y}{d\alpha} \right|_{\alpha=\bar{\alpha}}}$$

where N and δ_s are the natural frequency and logarithmic damping of the structure respectively. Using this formula the data in Fig. 2.4 can be used directly to calculate the transverse galloping speed for a wind at any specified incidence.

3.3. Critical Galloping Speed for Cross-Sectional Approximations.

An assessment can be made of the critical galloping speeds for the various shapes described in section 2 using the quasi-steady theory outlined in section 3.2. The fundamental natural frequency in bending of the mast is based on a Finite Element modal analysis carried out by W.S. Atkins, and corresponds to the first mode, illustrated in Fig. 3.3. The calculated natural frequency was 0.73Hz. The stability calculations assume an air density of 1.2kg/m^3 and, as explained in section 2.1, a damping ratio of 4%.

The stability calulations are summarised in Table 2, which identifies for each shape the mean incidence, slope of the transverse force graph, the critical velocity and the corresponding reduced velocity, given by $V_r = \frac{V}{Nh}$. Note that the data for the ellipses in Fig. 2.4 indicate stability at all angles, and are therefore omitted from Table 2. For supercritical flow conditions the calculated critical galloping speeds for all shapes are well in excess of the design speed (~45m/s at the top of the mast). The critical speed for the rounded square in subcritical flow is close to the design speed, however the predicted value corresponds to flow conditions which are well into the supercritical region in this case (see section 2.3) and hence should not be of concern. The corresponding reduced velocity values indicate that the quasi-steady theory is generally applicable, that is the critical galloping speeds are well separated from the speeds at which resonance due to vortex shedding would be expected. However the speed predicted for the shape formed from the eccentric circles will not be an accurate value due to the omission of compressibility effects. This latter prediction does indicate however that the shape is not expected to be unstable in galloping at speeds close to the design speed.

It must be stressed that the critical galloping speed depends strongly on the slope of the transverse force graph. Although an attempt has been made to represent the various features of the mast cross-section, differences in the separation characteristics can produce significant differences in the transverse force behaviour. More confidence in the stability assessment of the mast requires data to be made available for the actual cross-section. This data could be obtained from wind tunnel tests, the facilities being available within the Department of Aerospace Engineering at the University of Glasgow.

4. CONCLUSIONS.

From the assessment of the transverse galloping stability of the mast of the Tower Hotel, which is part of the Chicago Beach Resort Development, a number of conclusions can be drawn, and these are listed below.

- Aerodynamic data for the mast cross-sectional shape have not been found. A number of different shapes which exhibit some of the important features of the mast cross-section have been identified and the corresponding aerodynamic data found and processed.

- Both the structural data supplied by W.S. Atkins and the aerodynamic data for the cross-sectional approximations have been employed in the quasi-steady theory of transverse galloping stability. This theory has been extended from that reported by Vezza (1996) to accommodate wind speeds at non-zero angles of incidence.

- An assessment of the critical galloping speeds of the cross-sectional approximations indicates stability at all winds speeds likely to occur at the site of the Hotel. The estimates are considered to be conservative due to the neglect of both three dimensional flow at the tip of the mast and the possible underestimation of structural damping.

- Based on the various shapes investigated, there is strong evidence to suggest that the mast will not experience an instability due to transverse galloping. However, given the sensitivity of the transverse force characteristic to changes in the separation conditions, more confidence in this assessment requires aerodynamic data for the actual cross-section of the mast to be made available. This data could be obtained from a series of wind tunnel tests.

REFERENCES.

Coleman, S.A.; Davies, M.E.	1994	*Chicago Beach Resort Development - Wind Tunnel Tests.* BMT Report, Project No. 43049.
ESDU	1979	*Mean Fluid Forces and Moments on Cylindrical Structures: Polygonal Sections with Rounded Corners Including Elliptical Shapes.* Engineering Sciences Data Unit Item No. 79026.
Novak, M.; Tanaka, H.	1974	*Effect of Turbulence on Galloping Instability.* Proc. A.S.C.E., J. Eng. Mech. Div., vol. 100, EM1, p. 27-47.
Polhamus, E.C.	1958	*Effect of Flow Incidence and Reynolds Number on Low Speed Aerodynamic Characteristics of Several Noncircular Cylinders with Applications to Directional Stability and Spinning.* NACA TN 4176.
Richardson, A.S.	1986	*Bluff Body Aerodynamics.* J. Structural Engineering, vol. 112, p. 1723-1726.
Vezza, M.	1996	*Chicago Beach Resort Development - A Review of Galloping of Rectangular Prisms Pertinent to the Stability of the Tower Hotel External Frame.* G.U. Aero Report No. 9619.

Table 1. Mass Distribution of the Mast.

Bay No.	1	2	3	4	5	6
Mass per Unit Length (kg/m)	750	1876	1725	1895	1980	2201

Table 2. Summary of Galloping Stability Calculations.

Cross-Sectional Shape	Wind Incidence $\bar{\alpha}$ (deg)	Force Coeff. Slope $\left.\frac{dC_y}{d\alpha}\right\|_{\alpha=\bar{\alpha}}$ (rad^{-1})	Critical Velocity V_{crit} (m/s)	Reduced Velocity V_r
Rounded Square [1]	20	2.49	153.7	84.2
Rounded Square [2]	0	7.51	42.3	23.2
Rounded Rectangle	20	2.29	167.1	91.6
Eccentric Circles	12	0.79	429.5	235.3

1. supercritical Reynolds number
2. subcritical Reynolds number

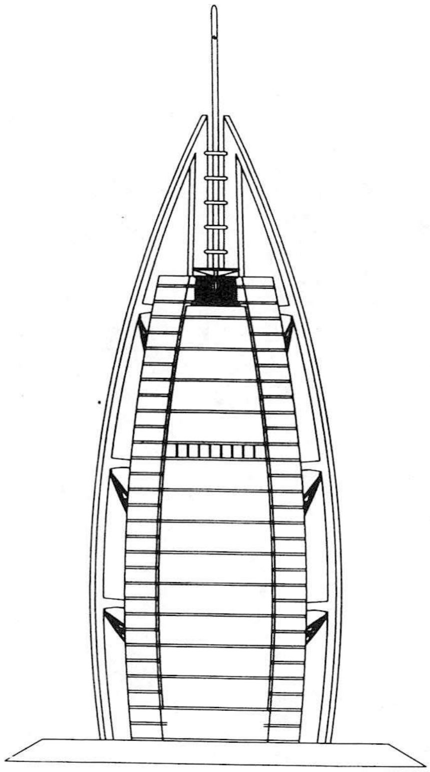

(a) Rear Elevation

(b) Side Elevation

Fig. 1.1. Diagram of Tower Hotel.

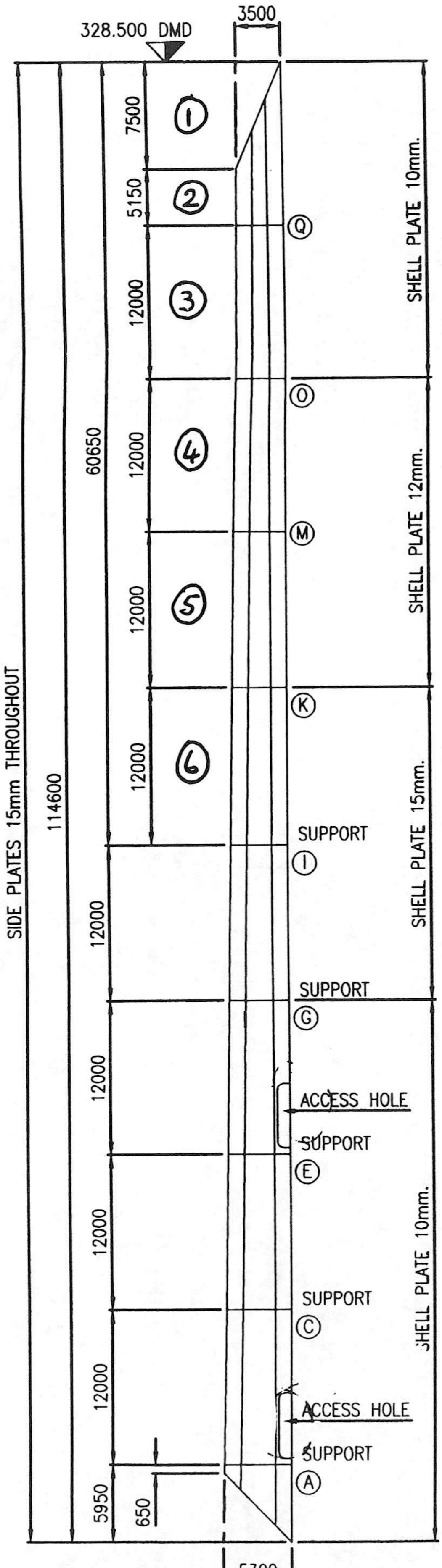

Fig. 2.1. Details of Mast Arrangement.

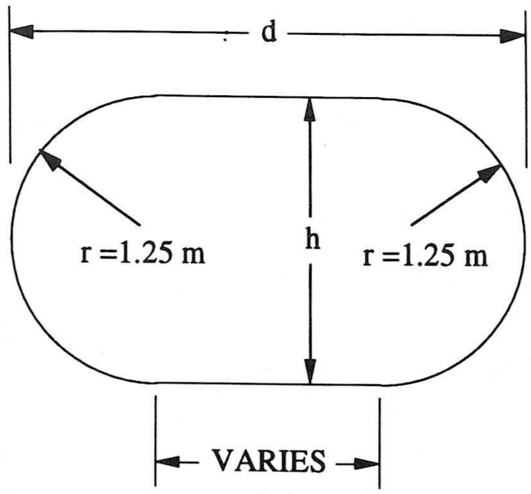

Fig. 2.2. Basic Form of Mast Cross-Section.

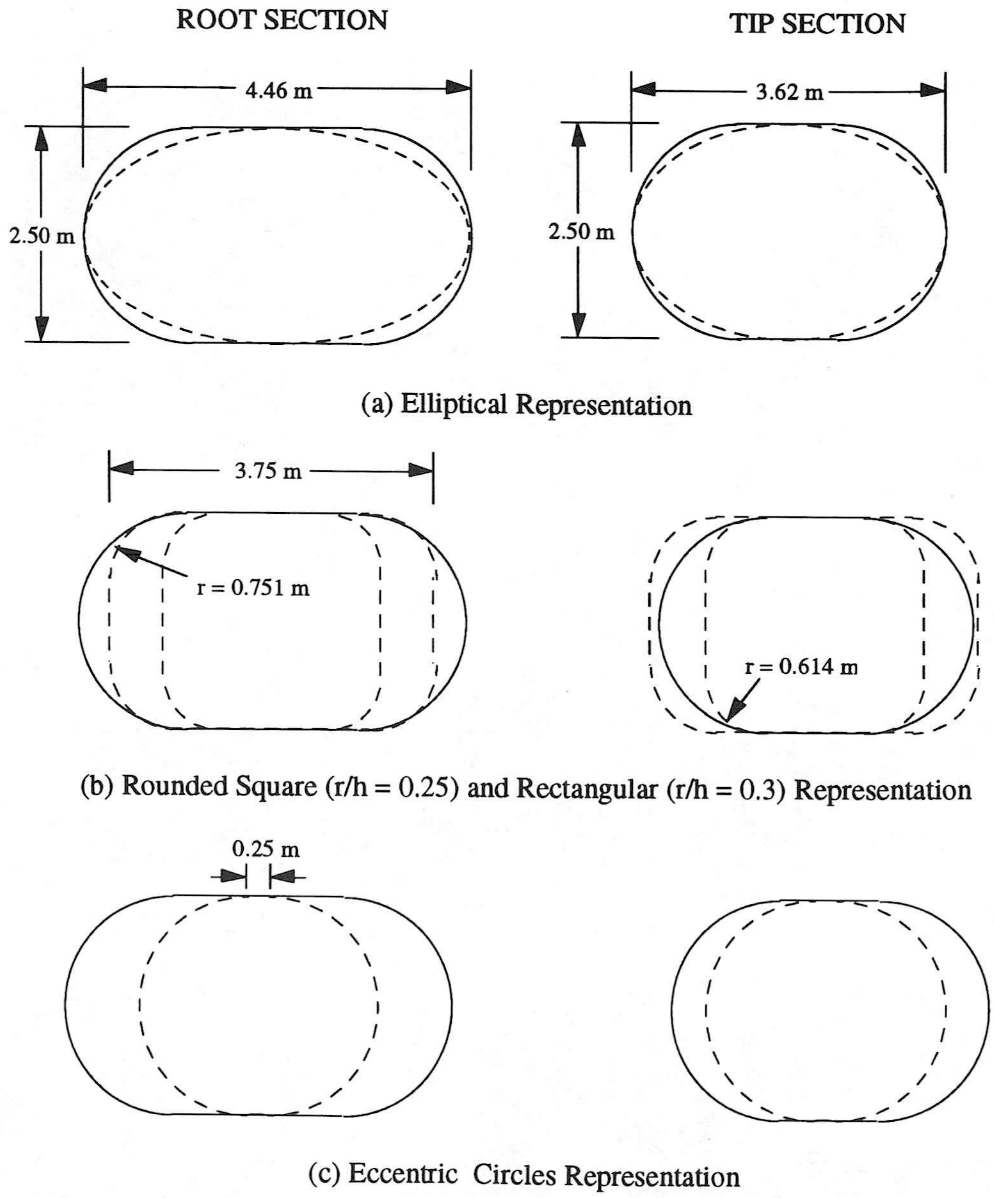

Fig. 2.3. Various Shapes Approximating the Mast Cross-Sections.

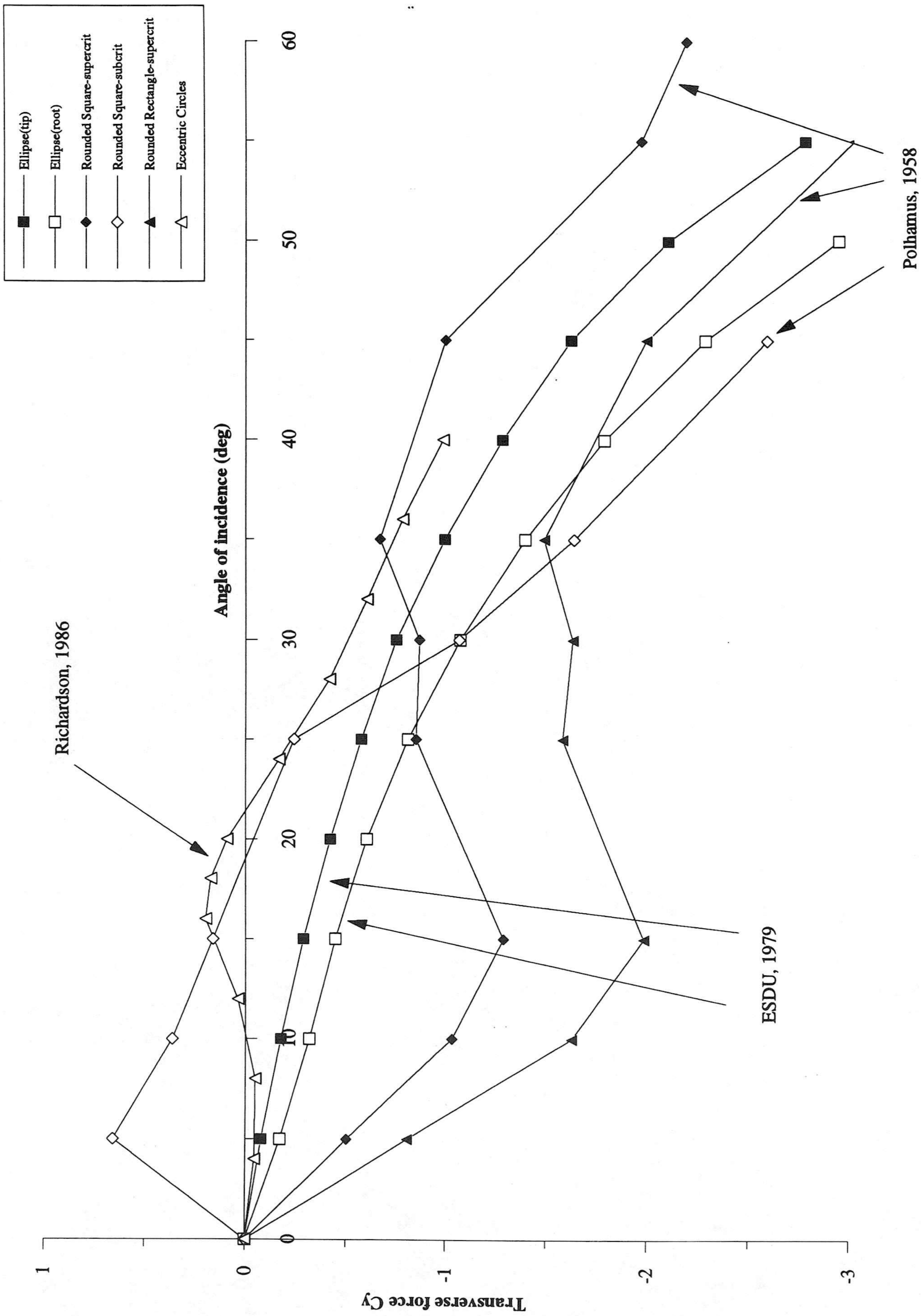

Fig. 2.4. Transverse Force Coefficient for Cross-Sectional Approximations.

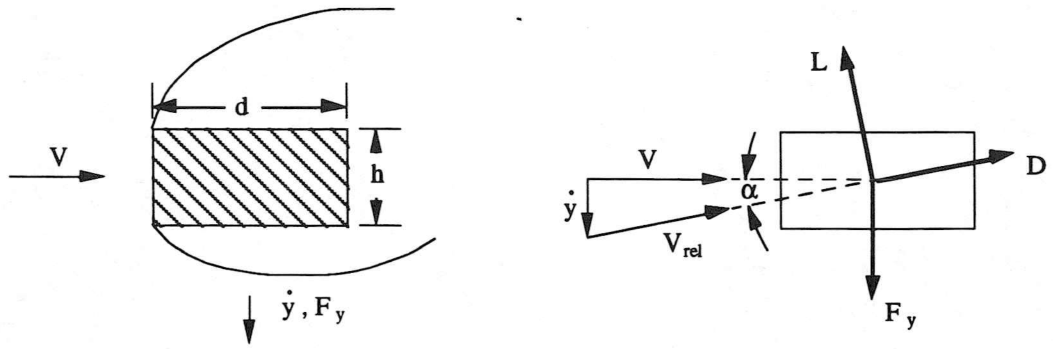

Fig. 2.5. Sign Convention for Transverse Force Data.

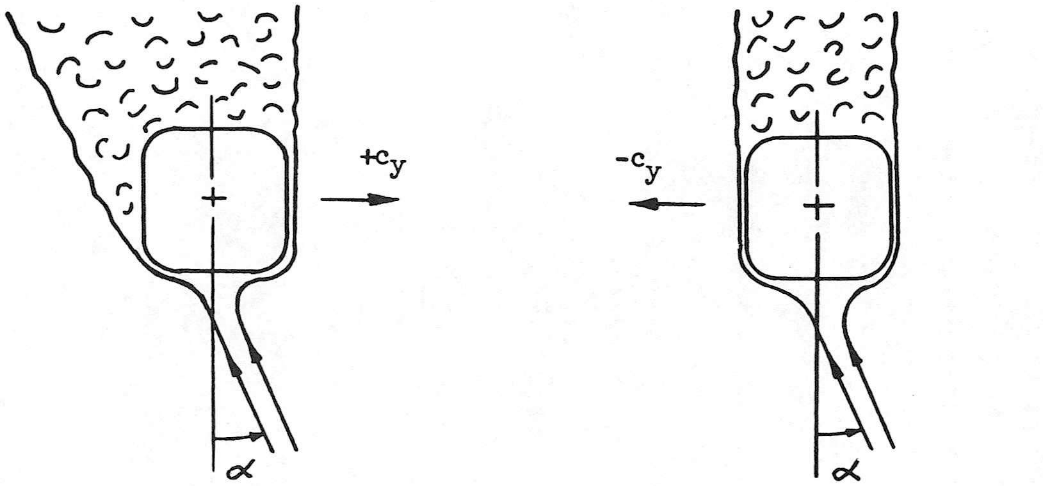

Fig. 2.6. Effect of Reynolds Number Region for Flow Past Rounded Bodies.

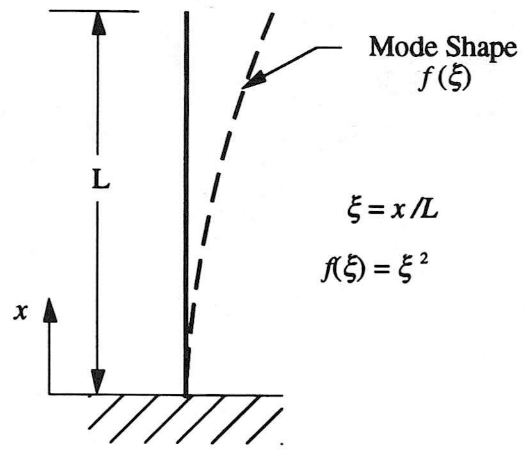

Fig. 3.1. Parabolic Mode Shape for Cantilever.

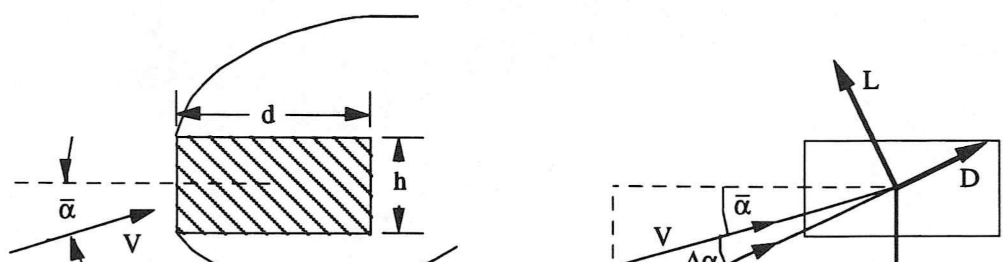

Fig. 3.2. Sign Convention for Wind at Non-Zero Incidence

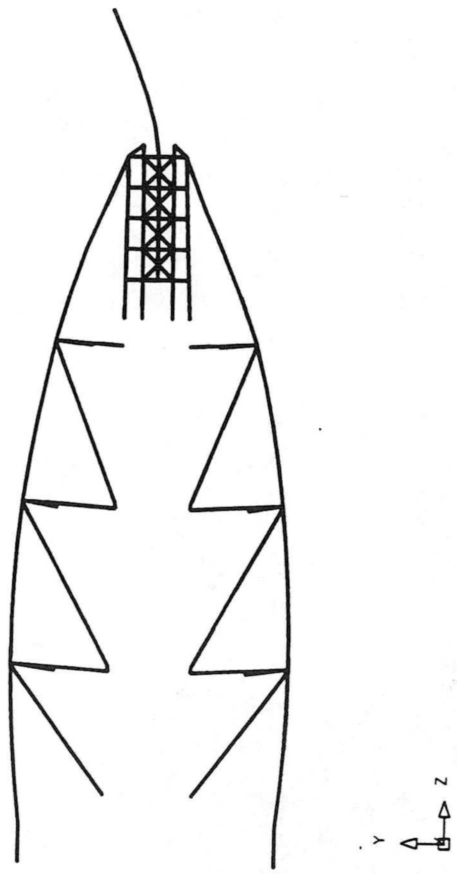

Fig. 3.3. Fundamental Mode Shape of Vibration for Mast.